

# Ion beam figuring of small optical components

**Thomas W. Drueding**  
Boston University  
College of Engineering  
Aerospace and Mechanical Engineering  
Department  
Boston, Massachusetts 02215

**Steven C. Fawcett**, MEMBER SPIE  
National Aeronautics and Space  
Administration  
Optical Fabrication Branch, EB53  
Marshall Space Flight Center, Alabama  
35812

**Scott R. Wilson**  
Sandia Systems Incorporated  
2655-A PanAmerican Freeway NE  
Albuquerque, New Mexico 87107

**Thomas G. Bifano**  
Boston University  
College of Engineering  
Aerospace and Mechanical Engineering  
Department  
Boston, Massachusetts 02215  
E-mail: [tgb@bu.edu](mailto:tgb@bu.edu)

**Abstract.** Ion beam figuring provides a highly deterministic method for the final precision figuring of optical components with advantages over conventional methods. The process involves bombarding a component with a stable beam of accelerated particles that selectively removes material from the surface. Figure corrections are achieved by rastering the fixed-current beam across the workpiece at appropriate, time-varying velocities. Unlike conventional methods, ion figuring is a noncontact technique and thus avoids such problems as edge rolloff effects, tool wear, and force loading of the workpiece. This work is directed toward the development of the precision ion machining system at NASA's Marshall Space Flight Center. This system is designed for processing small ( $\approx 10$ -cm diam) optical components. Initial experiments were successful in figuring 8-cm-diam fused silica and chemical-vapor-deposited SiC samples. The experiments, procedures, and results of figuring the sample workpieces to shallow spherical, parabolic (concave and convex), and non-axially-symmetric shapes are discussed. Several difficulties and limitations encountered with the current system are discussed. The use of a 1-cm aperture for making finer corrections on optical components is also reported.

*Subject terms:* ion figuring; optical fabrication.

*Optical Engineering* 34(12), 3565–3571 (December 1995).

## 1 Introduction

The final figuring step in the fabrication of an optical component involves imparting a specified contour to the surface. This can be an expensive and time-consuming step. The recent development of ion beam figuring provides a method for performing the figuring process with advantages over standard mechanical methods. Ion figuring has proven effective in figuring large optical components.<sup>1–7</sup>

The process of ion beam figuring removes material by transferring kinetic energy from impinging neutral particles. The process utilizes a Kaufman-type ion source, where a plasma is generated in a discharge chamber by controlled electric potentials.<sup>8</sup> Charged grids extract and accelerate ions from the chamber. The accelerated ions form a directional beam. A neutralizer outside the accelerator grids supplies electrons to the positive ion beam. It is necessary to neutralize the beam to prevent charging workpieces and to avoid bending the beam with extraneous electromagnetic fields. When the directed beam strikes the workpiece, material sputters in a predictable manner. The amount and distribution of material

sputtered is a function of the energy of the beam, material of the component, distance from the ion source to the workpiece, and angle of incidence of the beam. The figuring method described here assumes a time-invariant beam removal function, so that the process can be represented by a convolution operation. A fixed beam energy maintains a constant sputtering rate. This temporarily and spatially stable beam is directed perpendicular to the workpiece at a fixed distance. Desired contours are achieved by rastering the beam over the workpiece at varying velocities. A deconvolution is performed, using a series-derivative solution<sup>9</sup> developed for the system, to determine appropriate velocities as a function of beam position over the workpiece.

Early work on the ion figuring of optical components was performed by Gale.<sup>10</sup> This work was expanded at the University of New Mexico by Wilson et al.<sup>5–7</sup> The initial experiments involved figuring of 30-cm fused silica, Zerodur, and copper optics with a 2.54-cm ion beam source. Allen et al. developed an ion figuring system for large optics at Eastman Kodak.<sup>1–4</sup> The Kodak ion figuring system (IFS) is capable of processing components up to 2.5 m by 2.5 m using several ion sources of up to 15-cm diam. Other current research is being carried out at Oak Ridge National Laboratory. Their system is capable of figuring components up to 60 cm in diameter.<sup>11</sup> The new precision ion machining system

Paper 03124 received Dec. 7, 1994; revised manuscript received May 26, 1995; accepted for publication May 26, 1995.  
© 1995 Society of Photo-Optical Instrumentation Engineers. 0091-3286/95/\$6.00.

(PIMS) research facility at NASA's Marshall Space Flight Center is focused on the figuring of small ( $\approx 10$ -cm diam) optics using a 3-cm ion source. The experiments discussed here involved figuring 8-cm-diam fused silica and chemical-vapor-deposited SiC.

The two main advantages of the ion machining process are that it is noncontacting and highly predictable. The absence of contact eliminates the problems of tool wear and edge effects encountered in most standard grinding and polishing techniques. The process also avoids mounting and support-structure print-through and warping due to loading stresses on the workpiece. Holding beam parameters constant ensures beam stability and results in a predictable and highly deterministic removal process. This allows for rapid convergence of the process to required specifications, resulting in significant time and cost savings.

Issues of concern in the ion beam figuring process include beam stability, the surface properties of the workpiece, workpiece heating, and dwell-function computation. Beam stability affects the predictability and accuracy of the removal process, while workpiece surface properties and heating influence the effectiveness of the process. The effects on the surface roughness are reported in earlier work.<sup>12</sup>

## 2 PIMS Configuration

### 2.1 Equipment

The PIMS machining apparatus itself is constructed around a vacuum sputtering chamber. Fitted inside the chamber is a 3-cm, Kaufman filament-type ion source driven by a programmable power supply. A computer-controlled motion stage is fitted to the floor of the chamber, below the ion source. The workpiece holder is placed on the translation stage that provides translations and rotations of the workpiece. The motion of the system as well as the ion-source power supply is controlled by an 80386-based personal computer. In the configuration, the workpiece is moved and the ion beam source is held in a fixed position above the work area. The system is depicted in the computer model of Fig. 1.

Surface contour measurements are taken using a ZYGO Mark IVxp interferometer with a 4-in. aperture. For computing rastering parameters, the surface map is transferred to a personal computer. Surface roughness measurements are taken using a WYKO 3-D optical profilometer. The sample workpieces are circular and 80.0 mm in diameter.

### 2.2 Raster System

Two translation motors are used for  $x$ - $y$  motion, and a rotational motor for angular motion. These motors were purchased from Klinger Scientific Corporation. The translation motors are stepping motors with a 100-mm range and a maximum velocity of 0.3 mm/s. The velocity range required for the figuring process exceeds the maximum velocity of the translational motors. The rotational dc motor, with a maximum velocity of 15 rpm, provides sufficient tangential velocity for figuring. A workpiece holder attached to the motion system was designed to provide coverage of the motors to prevent heating and damaging of the motors from exposure to the beam.

The ion beam's operational center is determined using the  $x$ - $y$  motors. But in the figuring process the  $y$ -axis motor pro-

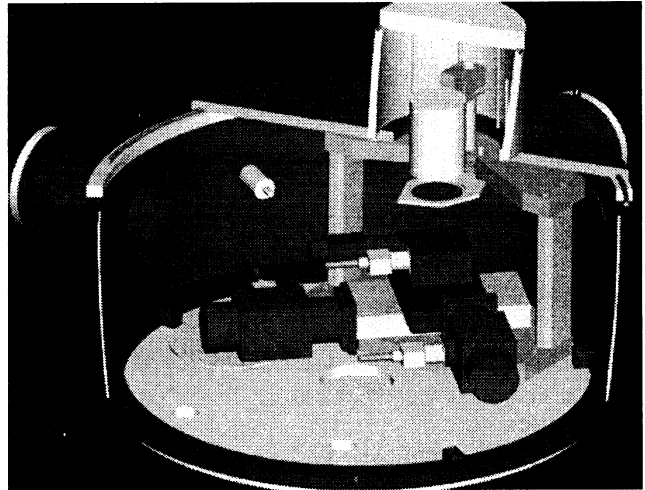


**Fig. 1** Solid model of the ion figuring system components. The ion source is supported on two posts above the translation and rotation stage assembly. These components are housed in a 1-m-diam, cylindrical vacuum chamber.

vides  $r$ -axis motion and the rotational motor provides  $\theta$  motion in polar coordinates. During figuring the beam center is rastered in concentric circle paths shown in Fig. 2. Concentric circle paths use only the rotational motor during beam operations and avoid the velocity limitations of the translational motors. Beginning with the outer ring, the beam is rotated around the center of the workpiece. When the ring is completed, the beam is automatically shut off and the  $r$ -axis motor incrementally bumps the beam center down to the next ring. The beam is subsequently reactivated and the process is repeated until completing the ring closest to the center of the workpiece. In the experiments the rings are separated by 4 mm. In addition, because the workpiece rotates under the beam, the beam center need only translate half the radius of the work area. This allows the system to accommodate larger optics—specifically, the 80-mm sample workpieces. Because the beam must cover an area at least 40 mm greater around the workpiece, the 100-mm range of the translation motors is insufficient to cover the work area of an 80-mm part. The sample workpieces used for initial experiments are also circular, making a polar coordinate system natural for the work area. A spiral rastering path was not attempted because of the difficulty in coordinating the translational and rotational motors while providing required varying tangential velocities.

### 2.3 Ion Beam Removal

The system uses a 3-cm, Kaufman filament-type ion source<sup>8</sup> from Ion Tech Incorporated. Argon gas provides the ions, and a typical beam current of 50 mA is used here for figuring. The source is controlled by a MPS-3000 power supply, also from Ion Tech. The power supply is in turn activated and monitored with the personal computer controlling the stage motion.

After installation it is necessary to determine the beam center relative to the stage coordinate system. To perform the computations<sup>9</sup> in the figuring process, the statistical moments of the static beam removal are required. A Gaussian

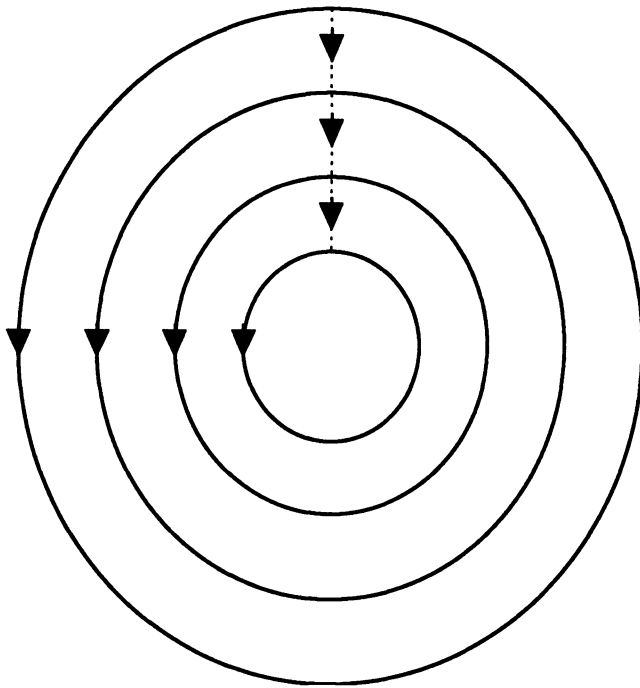


**Fig. 2** Rastering path of the beam center in the precision ion machining system.

function is used to model the beam removal, and the moments are subsequently computed from the functional model. The Gaussian beam function is characterized by its intensity, the peak removal rate  $\Gamma$ , and its width  $\omega$ :

$$B(x,y) = \Gamma \exp[-(x^2 + y^2)/\omega^2] \quad (1)$$

These parameters are determined experimentally by fitting the Gaussian function to data as explained below. The volumetric removal rate  $\gamma$  is a function of the two parameters:

$$\gamma = \Gamma \pi \omega^2 \quad (2)$$

For determining these parameters, the surface contour of the sample (close to flat) workpiece was initially measured with the interferometer. Subsequently, the sample was centered under the beam and machined for a known amount of time. The difference between the postmachining surface and the initial surface provides the removal distribution. The data are divided by the machining time to get a removal rate. The function parameters are then determined from the resulting data.

The beam function defined above is nonlinear in its parameters and requires the use of nonlinear fitting methods. But by taking the natural log of the expression, a linear relation is found:

$$\log B(x,y) = \log \Gamma - (x^2 + y^2)/\omega^2 \quad (3)$$

This linear relation is clarified by using related parameters:

$$H(x,y) = a + b(x^2 + y^2) \quad (4)$$

$$a = \log \Gamma, \quad b = -1/\omega^2$$

Standard numerical linear least-squares fitting routines de-

termine the function parameters.<sup>13</sup> This still leaves a lot of possible ways to complete the fitting, including various ways of weighting the data. For example, the center of the beam removal can be defined as the maximum point or the centroid of the removal data; or alternatively the center can also be determined as free parameters for the fitting routine. Likewise, the peak removal rate can be defined as the maximum data height or as a free parameter.

Two experiments to determine the beam removal function were performed using the parameters in Table 1. In the first experiment a peak removal of 2920 nm resulted after 20 min of machining. During the second experiment the same piece was machined for an additional 20 min and underwent a peak removal of 6370 nm. A beam removal width parameter, defined above, of 25 mm and a peak removal of 160 nm/min were finally used for the model. The function is shown in Fig. 3 over an 80- by 80-mm area. The two experiments also demonstrate that the removal rates in the two 20-min periods were similar but not identical. The large beam width compared to the 80-mm diameter of the sample workpiece makes the figuring of these smaller optics more difficult than that of larger optical components.

### 3 Processing Experiments

#### 3.1 Experimental Procedure

Initial experiments involved figuring prepolished fused silica and chemically-vapor-deposited (CVD) SiC samples. The samples are circular, 80.0 mm in diameter, and 6.35 mm thick. All the samples were prepolished to  $\leq 10\text{-\AA}$  surface roughness.

For each figuring experiment, five surface roughness measurements and two surface contour measurements are recorded before machining. A surface contour map measured by the interferometer is transferred to a personal computer for the following computations. The desired contour is subtracted from the measured surface map to provide a map of material to remove. According to the previously discussed deconvolution method,<sup>9</sup> a function (weighted polynomial series) is fitted to the *removal map*. For these experiments, a

**Table 1** Ion-source operating parameters.

Parameter	Value
Discharge Current	0.6 A
Discharge Voltage	40 V
Beam Current	50 mA
Beam Voltage	1000 V
Accelerator Current	2 mA
Accelerator Voltage	200 V
Neutralizer Current	50 mA
Filament Current	4.1 A
Source Distance	8 cm

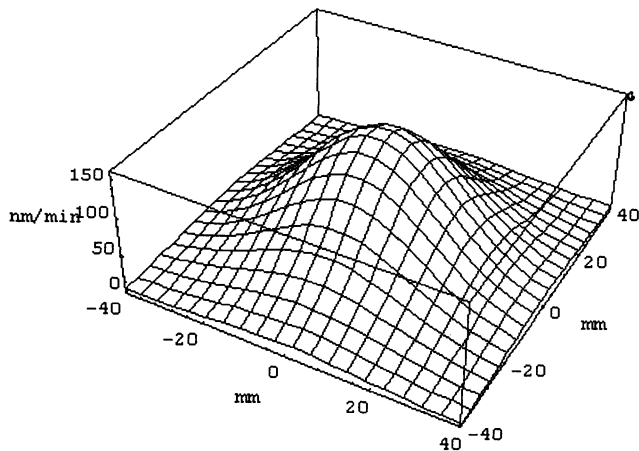


Fig. 3 Ion beam removal function.

21-term expansion is fitted to the surface. The deconvolution is performed using this series to produce the corresponding series expansion for the *dwell function* and rastering velocities.

During the figuring process the stage is moved under the beam. The motion rasters the beam center across the work area in concentric circular paths, and the angular velocities in each ring are varied according to the dwell function. Between rings the ion beam source is shut off to avoid removing material as the beam is translated to the next ring. In the initial experiments, each figuring process is begun with the outermost ring 10 mm beyond the workpiece, because removal is expected even when the beam is not centered directly on a point on the workpiece. It was later determined that it is necessary to begin with the ring at least 40 mm beyond the workpiece to allow for the width of the actual beam. Thirteen rings are used, 4 mm apart, beginning at 50 mm and ending at 2 mm from the center of the workpiece. Each ring is broken into segments no longer than 4 mm. The velocity associated with each segment is computed by multiplying the dwell-function value at the center of the segment by the characteristic width (4 mm) and taking the reciprocal. This provides a tangential velocity value that is converted to an angular velocity for the rotation motor. After machining, the surface contour is remeasured and the relative improvement of the contour is evaluated. Five surface roughness measurements are recorded for each sample after all machining experiments on that sample.

### 3.2 Contour Figuring Results

The results of the process for 12 cases are shown in Table 2. Using a 3-cm-diam ion source, 10 fused silica samples were figured to spherical, parabolic (concave and convex), and skewed shapes with approximately 4  $\mu\text{m}$  of sag. Figure 4 shows the results for the 10 fused silica cases. Initial deviations from the desired figures ranged from 500 to 2000 nm rms, and the ion figuring process corrected the figures to an average of 365 nm rms error. The average convergence ratio over the 10 cases was 4.10, with typical values of around 3.0.

The first case involved imparting a shallow parabola (4  $\mu\text{m}$  of sag) on a flat fused silica sample that had an initial

**Table 2** Results of ion beam figuring of 8-cm fused silica and silicon carbide samples. A 3-cm beam ion source created parabolic, spherical, and saddle figures. In addition, a 1-cm aperture on the beam was used to correct a flat fused silica sample. The initial and final rms deviation from the desired figure is shown for each case. The convergence ratio represents the effectiveness of the process and is the initial divided by the final rms deviation.

Case	Target Profile	Initial rms	Final rms	Convergence
<b>Fused Silica (3 cm Beam Width)</b>				
1	Parabola (radius: 100,000 mm)	1138 nm	80 nm	14.20
2	Parabola (radius: -100,000 mm)	1071 nm	434 nm	2.47
3		1170 nm	380 nm	3.08
4		858 nm	359 nm	2.39
5	Sphere (radius: 100,000 mm)	2279 nm	419 nm	5.44
6		817 nm	256 nm	3.19
7	Skewed (radius: 160,000 mm)	933 nm	638 nm	1.46
8		934 nm	456 nm	2.05
9	Skewed (radius: 140,000 mm)	934 nm	261 nm	3.58
10	Saddle (radius: 300,000 mm)	770 nm	246 nm	3.13
	<i>Averages</i>		353 nm	4.10
<b>Silicon Carbide (3 cm Beam Width)</b>				
11	Saddle	982 nm	324 nm	3.03
<b>Fused Silica (1cm Beam Width)</b>				
12	Flat	59 nm	24 nm	2.44

surface error of 1138 nm rms from the parabola. This was reduced to 80 nm rms after machining. The initial peak-valley error of 4093 nm was reduced to 390 nm. The final shape is shown in Fig. 5, and the deviation is shown in Fig. 6. The process took a total of 121 min of beam operation, and the surface roughness before and after machining was less than 10  $\text{\AA}$  rms. Experiments to impart convex parabolas were also conducted; since in them more material is removed along the outside of the workpiece, a significant amount of material removal is expected when the beam is not centered on the workpiece. Other experiments implemented skewed saddle-like shapes, demonstrating the capability of non-axially-symmetric corrections. The skewed shape is defined as follows:

$$z = \frac{x^2 + y^2 + xy}{4 \times \text{radius}} \quad (5)$$

For example, the final contour of the sample in case 9 is shown in Fig. 7; the deviation, in Fig. 8. The sample had an initial surface deviation of 934 nm rms from a saddle that was corrected to 261 nm rms in 91 min of figuring. Also, a skewed contour was figured on a CVD silicon carbide sample, improving the figure error from 982 to 324 nm rms. Additional iterations failed to improve the workpiece contours

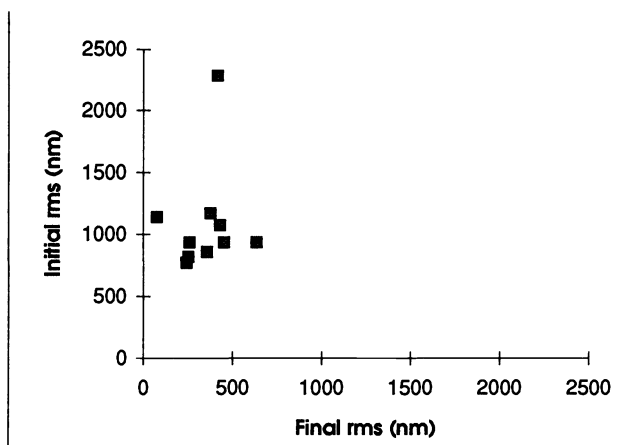


**Fig. 4** Results of ion figuring of the 10 fused silica samples with the open, 3-cm source, displaying final rms figure error versus initial rms figure error. The slope from the origin to a point is the convergence ratio of that case.

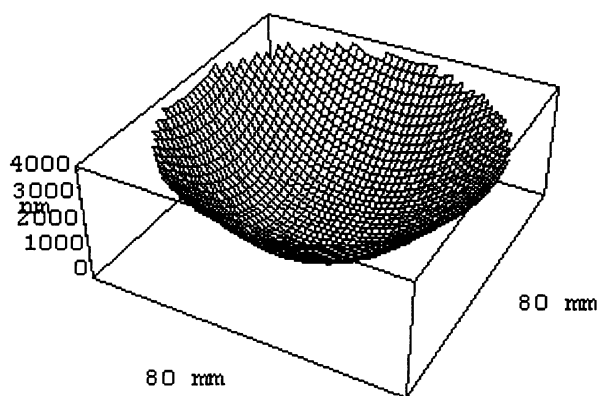


**Fig. 5** The final surface contour of part in case 1 after figuring to impart parabolic contour. The surface shown deviates from the desired contour by 80 nm rms.

because of an apparent variation in the beam removal that was discovered later and is discussed below.

Occasionally the neutralizing filament failed during a figuring process. Then the process was stopped, the filament replaced, and the process restarted at the point where the failure occurred. No adverse effects were observed from the interruption.

Several cases are not shown where the stage motors unexpectedly stopped and the beam dwelled at a point for extended periods of time. These samples were unrecoverable without repolishing because correcting for a deep hole requires removing a large amount of surrounding material, and excessive processing time. This problem was traced to the software controlling the motors and was corrected.

The figuring experiment results indicated a higher removal rate at the center of the workpiece than at the edges. The variation in beam removal appeared to be axially symmetric about the center of the workpiece, and subsequent iterations failed to improve the surface contours because of this variation in the beam removal. Later modeling showed that the initial outermost ring needed to be started further away from the edge of the optic to allow for the broad beam removal

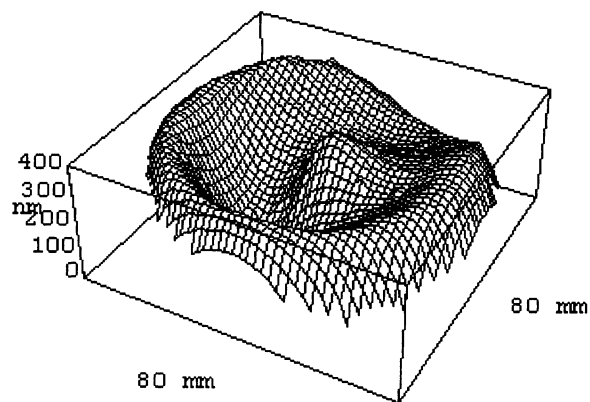


**Fig. 6** The final deviation from the desired in case 1, 80 nm rms.

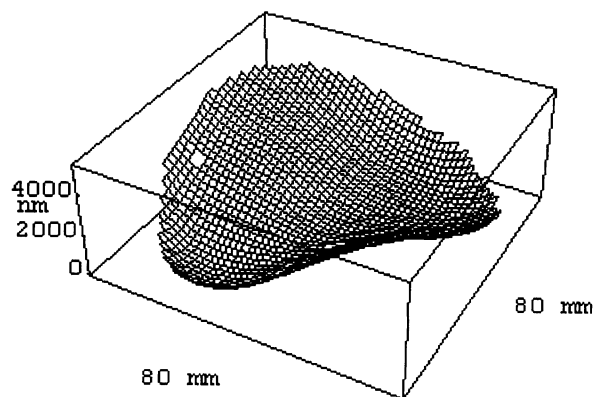


**Fig. 7** The final surface contour of part in case 9 after figuring to impart a saddle contour. The surface shown deviates from the desired contour by 261 nm rms.

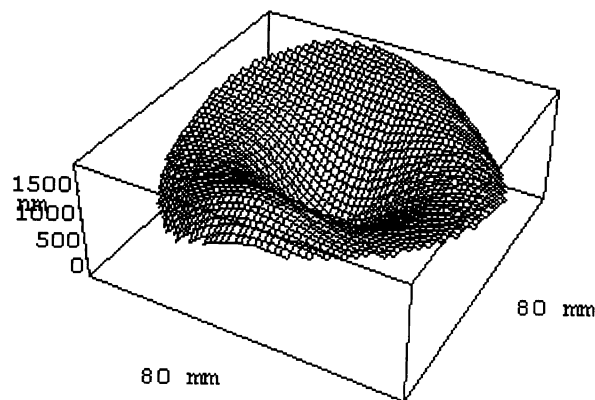


**Fig. 8** The final deviation from the desired in case 9, 261 nm rms.

function. The modeling also showed that beam-optic misalignment does not cause this type of error. With the 25-mm beam width the work area must extend at least 40 mm beyond the workpiece.

### 3.3 Surface Roughness

Five roughness measurements were made on each workpiece prior to any machining. After all machining on each work-

piece, five additional measurements were taken to determine the effects of the figuring process. The initial and final average measurements are shown in Table 3 along with the total amount of time the sample was machined. The three cases shown are samples for which the complete history is known and that did not experience any defects from sources other than ion figuring. The typical figuring process removes an average of 2  $\mu\text{m}$  of material per hour. Some of the samples were machined several times, but measurements were only taken after all machining was completed. None of the samples experienced significant increases in surface roughness. This also indicates that the samples were carefully polished and contained little subsurface damage.<sup>12</sup>

Some samples experienced severe, visible defects. It was discovered that previously sputtered material had formed a coating on the roof of the vacuum chamber. This material would flake off and drop on the workpiece during machining. Ions would preferentially remove material along the edges of the flakes and when the flaked material finally sputtered away, the holes along the edges would coalesce. The defects stopped appearing once the coating on the chamber ceiling was noticed and removed.

### 3.4 Beam Aperture Experiment

A 1-cm aperture was installed in the ion source to attempt higher-frequency corrections. A simple nonmagnetic stainless steel annulus is used for the aperture. The aperture is placed inside the source and rests on extraction grids. It is necessary to reduce the beam current, and therefore the peak removal rate, to achieve a stable beam with the aperture in place. The resulting beam removal was still Gaussian-shaped, but it had a greatly reduced volumetric removal rate, both because the overall width (footprint) was smaller and the peak removal was reduced. Experimentally determined beam parameters (assuming a Gaussian function as in Sec. 2.3) are shown in Table 4. The volumetric removal rate of the 1-cm apertured beam is 20 times less than the open source. This reduced removal rate makes the aperture source useful only for small (less than 100 nm rms) corrections.

The apertured ion beam source was used to improve a single flat fused silica sample with an initial surface error of 59 nm rms. The process took 138 min and reduced the surface contour to 24 nm rms from flat. The surface roughness measured before and after machining was less than 10 Å rms. The aperture could be used to make finer corrections on optical components but is limited by the reduced volumetric removal rate.

## 4 Conclusion

The precision ion machining system was successful in figuring 8-cm-diam fused silica and chemical-vapor-deposited SiC samples. The 12 cases are summarized in Table 2 for figuring to spherical, parabolic (concave and convex), and non-axially-symmetric shapes. A 1-cm aperture was used for correcting a near-flat, fused silica sample. Small apertures are useful for making finer corrections on optical components, but their use is limited by the reduced volumetric removal rate. Subsequent iterations failed to improve surface contours because of an apparent nonconstant removal that occurred because insufficient area was covered by the ion beam during machining. None of the workpieces experienced significant

**Table 3** Initial and final surface roughness measurements for three cases.

Case	Initial rms (Angstroms)	Final rms (Angstroms)	Process Time
1	9.6	10.1	121 min
2	8.9	12.1	328 min
3	8.6	10.2	187 min

**Table 4** Gaussian modeled ion beam parameters.

Source Diameter	3 cm	1 cm
Distribution Width, $\omega$	160 nm/min	42 nm/min
Peak Rate, $\Gamma$	25 mm	11 mm
Volumetric Rate, $\gamma$	0.1 $\pi$ mm <sup>3</sup> /min	0.005 $\pi$ mm <sup>3</sup> /min

increases in surface roughness, although severe defects appeared on some samples, caused by flakes of previously sputtered material dropping on the sample during the process.

The proposed processing technique shows promise as a viable alternative to conventional fabrication techniques in the production of ceramic mirror components. A small ion machining facility at NASA's Marshall Space Flight Center has been established, and successful figuring experiments have been carried out.

### Acknowledgments

This work was sponsored by NASA, and the authors would like to express their gratitude to the following people for their support of the project: Robert Rood, James Bilbro, Charles Jones, and Joseph Randall. We would also like to thank Jon Fleig of Tropel Inc. for insight that assisted writing this paper.

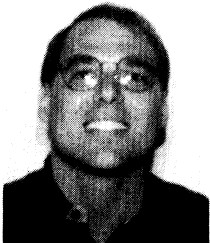
### References

1. L. N. Allen, J. J. Hannon, and R. W. Wambach, "Final surface error correction of an off-axis aspheric petal by ion figuring," in *Advances in Fabrication and Metrology for Optics and Large Optics*, Proc. SPIE 1543, 190–200 (1991).
2. L. N. Allen and R. E. Keim, "An ion figuring system for large optics fabrication," in *Current Developments in Optical Engineering*, Proc. SPIE 1168, 33–50 (1989).
3. L. N. Allen, R. E. Kiem, and T. S. Lewis, "Surface error correction of a Keck 10 m telescope primary segment by ion figuring," in *Advances in Fabrication and Metrology for Optics and Large Optics*, Proc. SPIE 1531, 195–204 (1991).
4. L. N. Allen and H. W. Romig, "Demonstration of an ion figuring process," in *Advances in Fabrication and Metrology for Optics and Large Optics*, Proc. SPIE 1333, 22–33 (1990).
5. S. R. Wilson, "Ion beam figuring of optical surfaces," Master's Thesis, Univ. of New Mexico, Albuquerque (1987).
6. S. R. Wilson and J. R. McNeil, "Neutral ion beam figuring of large optical surfaces," in *Current Developments in Optical Engineering*, Proc. SPIE 818, 320–323 (1987).
7. S. R. Wilson, D. W. Riecher, and J. R. McNeil, "Surface figuring using neutral ion beams," in *Advances in Fabrication and Metrology for Optics and Large Optics*, Proc. SPIE 966, 74–81 (1988).
8. H. R. Kaufman, P. D. Reader, and G. C. Isaacson, "Ion sources for ion machining applications," *AIAA J.* 15(6), 843–847 (1977).
9. T. W. Drueding, T. G. Bifano, and S. C. Fawcett, "Contouring algorithm for ion figuring," *Precision Eng.* 17(1), 10–21 (1995).

10. A. J. Gale, "Ion machining of optical components," *J. Opt. Soc. Am.* **68**(10), 1445-1446 (1978).
11. C. M. Egert, "Roughness evolution of optical materials induced by ion beam milling," *Proc. SPIE* **1752**, 63-72 (1992).
12. S. C. Fawcett, T. W. Drueding, and T. G. Bifano, "Neutral ion figuring of CVD SiC," *Opt. Eng.* **33**(3), 967-974 (1994).
13. W. H. Press, B. P. Flannery, S. A. Teukolsky, and W. T. Vetterling, *Numerical Recipes in C*, Cambridge Univ. Press, Cambridge (1992).



**Thomas W. Drueding** received a BS in aerospace engineering and an MS in electrical, both from Boston University. After achieving his BS, he worked in research involving satellite remote sensing for atmospheric characterization. He returned to Boston University for his MS and contributed to a major project in image processing, specifically medical imaging. He has performed extensive work in mathematical deconvolution techniques and control theory. Dr. Drueding recently completed his PhD in mechanical engineering at Boston University under the National Aeronautics and Space Administration Graduate Student Research Program. His research is in the area of ion beam machining.

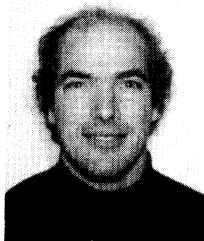


**Steven C. Fawcett** received his PhD in mechanical engineering from North Carolina State University in 1991. His primary research was in precision fabrication of optical materials. He has extensive experience in ion fabrication techniques, single-point diamond turning, optical metrology, ductile-regime grinding, and sensor and actuator development. Dr. Fawcett was formerly a research engineer for NASA Marshall Space Flight Center's Optical

Fabrication Branch, where he managed fabrication of relay optics for a composite infrared spectrometer. He is currently employed by Summit Technology Incorporated, of Waltham, Massachusetts.



**Scott R. Wilson** attended the University of New Mexico, receiving an MSEE (computer engineering) in 1987 and a PhD (electrical engineering) in 1991, both dealing with development of physical and computational technology for ion beam figuring. His research areas include image processing, computer architecture, physical electronics, optical fabrication and metrology, and semiconductor device fabrication and measurement technology. He is currently president and cofounder of Sandia Systems, Inc., in Albuquerque, New Mexico, specializing in ion beam processing and semiconductor metrology instrumentation.



**Thomas G. Bifano** received BS (1980) and MS (1983) degrees in mechanical engineering and materials science from Duke University and a PhD (1988) in mechanical engineering from North Carolina State University. Since joining the faculty of Boston University in 1988, Professor Bifano has developed an internationally known research program to study ultraprecision machining. He directs the Boston University Precision Engineering Research Laboratory, where he oversees currently active projects on ion machining of ceramics, ceramic hard-disk substrate fabrication, and silicon micromachining of deformable mirror systems.